

Effects of doping and magnetic field on the half-metallic electronic structures of $\text{La}_{1-x}\text{Ba}_x\text{MnO}_3$

S. J. Youn and B. I. Min

Department of Physics, Pohang University of Science and Technology, Pohang 790-784, Korea

(Received 5 November 1996; revised manuscript received 27 June 1997)

To deduce systematic trends in electronic and magnetic properties of colossal magnetoresistance (CMR) manganese oxides, we have investigated electronic structures of $\text{La}_{1-x}\text{Ba}_x\text{MnO}_3$ with varying doping concentration. Assuming a virtual solid of LbMnO_3 , where Lb stands for a virtual atom with a fractional atomic number between La and Ba, we have studied effects of the doping and the magnetic field on the electronic structures of $\text{La}_{1-x}\text{Ba}_x\text{MnO}_3$. It is found that the $\text{La}_{1-x}\text{Ba}_x\text{MnO}_3$ system is half metallic in the doping range of $x > 0.33$, and that it becomes half metallic even for $x < 0.33$ by applying the magnetic field. The half-metallic property in the presence of the magnetic field is discussed in relation to the observed CMR effect in doped LaMnO_3 systems. [S0163-1829(97)01043-6]

LaMnO_3 is an antiferromagnetic insulator with a distorted perovskite structure.^{1,2} When doped with divalent cations such as Ca, Sr, or Ba, it undergoes a phase transition to the metallic state and becomes ferromagnetic. Zener³ has explained these simultaneous metallic and magnetic phase transitions in doped LaMnO_3 in terms of the double exchange mechanism.⁴ Interest in this system has been revived recently due to observation of huge negative magnetoresistance (MR) phenomena in $\text{La}_{1-x}\text{Ca}_x\text{MnO}_3$ ($0.2 < x < 0.5$), so called, colossal magnetoresistance (CMR).⁵ The order of magnitude of MR value in $\text{La}_{1-x}\text{Ca}_x\text{MnO}_3$ is larger by several orders than that of giant MR magnetic multilayer systems. To explain these anomalous transport phenomena, many attempts have been made based on the double exchange Hamiltonian.⁶⁻⁸ However, Millis *et al.*⁹ pointed out that the double exchange alone could not explain the very large resistivity of the insulating phase for $T > T_c$, and so that the electron-phonon interaction arising from the Jahn-Teller splitting of Mn e_g states should be taken into account for extra physics.

There are several electronic structure calculations reported on undoped LaMnO_3 .¹⁰⁻¹³ Electronic structures for doped $\text{La}_{1-x}\text{Ba}_x\text{MnO}_3$ were also studied by Hamada *et al.*¹⁴ at $x=0.5$ by employing the virtual crystal approximation, and for $\text{La}_{1-x}\text{Ca}_x\text{MnO}_3$ by Pickett and Singh¹³ at $x=0, \frac{1}{4}, \frac{1}{3}$, and 1 by employing a large supercell calculation for $\frac{1}{4}$ and $\frac{1}{3}$. More sophisticated calculation using the coherent potential approximation was made by Butler *et al.*¹⁵ on $\text{La}_{0.67}\text{Ca}_{0.33}\text{MnO}_3$. Hamada *et al.* obtained a half-metallic ferromagnetic band structure for $x=0.5$. Note, however, that $\text{La}_{1-x}\text{Ca}_x\text{MnO}_3$ at $x=0.5$ is not a ferromagnetic metal but an antiferromagnetic insulator of CE type.¹ Pickett and Singh¹³ found that, in the assumed ferromagnetic phase, CaMnO_3 is a half metal whereas LaMnO_3 is nearly half metallic, and that there might be a metal-half-metal transition at an intermediate doping concentration. They also suggested that the half-metallic nature of $\text{La}_{1-x}\text{Ca}_x\text{MnO}_3$ is responsible for the CMR phenomena. More recently, effects of cationic disorder on the transport properties were also examined by Pickett and Singh¹⁶ with the virtual crystal approximation.

In this study, we have investigated electronic structures of $\text{La}_{1-x}\text{Ba}_x\text{MnO}_3$ at a general doping concentration, especially

for $0.2 < x < 0.5$ where $\text{La}_{1-x}\text{Ba}_x\text{MnO}_3$ is a ferromagnetic metal. $\text{La}_{1-x}\text{Ba}_x\text{MnO}_3$ is the first reported giant MR system in manganites with $MR = \{[\rho(H) - \rho(0)]/\rho(H)\} = 150\%$ at $x = \frac{1}{3}$.¹⁷ We have also examined effects of the magnetic field on the electronic structures in this system. We have found that $\text{La}_{1-x}\text{Ba}_x\text{MnO}_3$ becomes half-metallic depending on the doping concentration and also by applying the magnetic field. We have discussed the correlation between the half-metallic nature and the observed CMR phenomena in doped LaMnO_3 systems.

To investigate effects of the doping and the magnetic field in $\text{La}_{1-x}\text{Ba}_x\text{MnO}_3$, we have performed the linear muffin tin orbital band structure calculation on a virtual compound LbMnO_3 . To simulate $\text{La}_{1-x}\text{Ba}_x\text{MnO}_3$, a virtual compound LbMnO_3 is considered, where Lb represents a virtual atom with an intermediate fractional atomic number $Z = 56x + 57(1-x)$ between La and Ba. Since the hole doping with divalent atom corresponds to reducing the average number of electrons at the La site, the effect can be simulated by reducing the the number electrons at the La site. We have used the linearly interpolated lattice constant for LbMnO_3 at intermediate doping concentration. This approximation is, of course, a very primitive one, but in this way, a trend of electronic structures of $\text{La}_{1-x}\text{Ba}_x\text{MnO}_3$ for general x can be investigated.

Both CaMnO_3 and BaMnO_3 are half-metallic ferromagnets at the equilibrium lattice constants, that is, metallic in the majority spin channel and insulating in the minority spin channel. In contrast, LaMnO_3 is a normal metal at the equilibrium lattice constant (see the inset of Fig. 1). But notice that it is nearly half metallic. Indeed, if the lattice constant is enlarged a little bit, LaMnO_3 becomes half metallic too. Like LaMnO_3 , LbMnO_3 at low doping concentration is just a normal metallic ferromagnet. However, by increasing the doping concentration, it becomes half metallic. This behavior can be understood in the context that the hole doping plays a role of shifting down the Fermi level so as to produce a half metal. However, the band shift occurs in a nonrigid way. In Fig. 1, the variation of the energy gap between the conduction band bottom (CBB) and valence band top (VBT) of the minority spin of LbMnO_3 is plotted as a function of doping

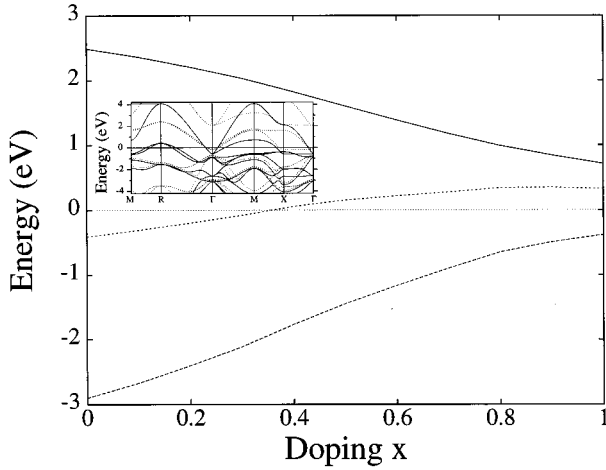


FIG. 1. Energy gap of the minority spin band vs doping concentration x in $\text{La}_{1-x}\text{Ba}_x\text{MnO}_3$ system. Dotted, dashed, and solid lines represent, respectively, the conduction band bottom (CBB), the valence band top (VBT), and the energy gap between the CBB and the VBT of the minority spin. In the inset, the band structure of the ferromagnetic cubic phase of LaMnO_3 is plotted. Majority and minority spin bands are represented by solid and dotted lines, respectively.

concentration. It is seen that both the CBB and VBT shift up in energy, and the energy gap decreases as doping increases, from 2.49 eV at $x=0$ to 0.71 eV at $x=1$. Half-metal results when the VBT is below E_F and the CBB is above E_F . Thus Fig. 1 shows that $\text{La}_{1-x}\text{Ba}_x\text{MnO}_3$ becomes half-metallic for $x > 0.33$.

Figure 2 shows the density of states (DOS) at $x=0.2$ and $x=0.4$. DOS at $x=0.2$ consists of six main peaks labeled as A to F. O- s and La- $5p$ bands located at -19 eV and -16.5 eV, respectively, are not shown in the figure. A and B peaks come from the hybridization between O- p , La- d , and Mn- d

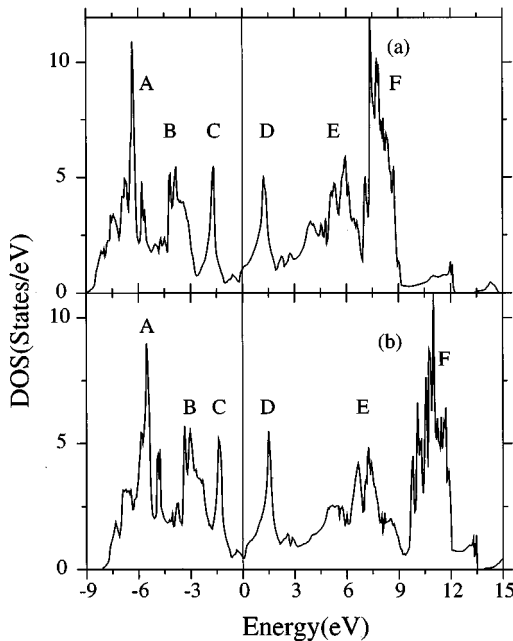


FIG. 2. Total DOS of LbMnO_3 at (a) $x=0.2$ and (b) $x=0.4$.

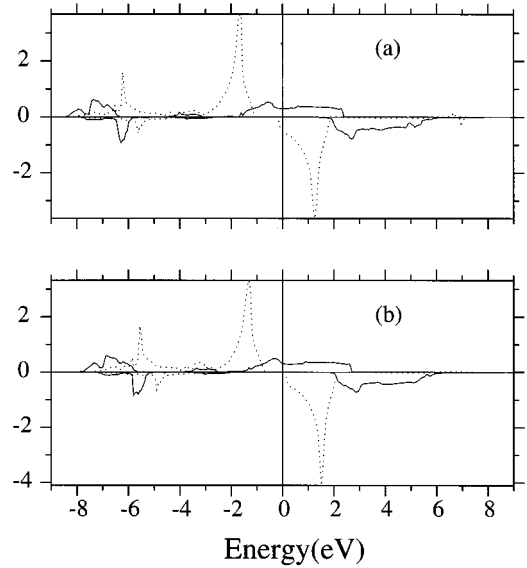


FIG. 3. Partial DOS (states/eV) of LbMnO_3 for t_{2g} and e_g symmetries at (a) $x=0.2$ and (b) $x=0.4$. Solid line and dotted line represent DOS of e_g and t_{2g} symmetry, respectively.

bands. C and D correspond to the DOS of the t_{2g} bands of Mn- $d\uparrow$ and Mn- $d\downarrow$ electrons, respectively. Separation between the two peaks represents the exchange splitting Δ_x of Mn- d band, which is about 3.0 eV at $x=0.2$ and nearly constant with varying x . E and F peaks correspond to La- d and La- f bands, respectively. It is the peak F that is most susceptible to doping concentration. The F peak shifts up by 3.0 eV as x changes from 0.2 to 0.4. A and B peaks also move up to E_F . Accordingly, the valence band width decreases as x goes from 0.2 to 0.4. It is also noticeable that E_F is located at the valley between two large peaks of DOS.

According to Zener's double exchange mechanism, Mn- d electrons are divided into two groups. Fully occupied t_{2g} electrons constitute localized moment, and the ferromagnetic coupling between these localized moments are carried by itinerant e_g electrons. Figure 3 shows a partial DOS of Mn- d electrons decomposed by t_{2g} (dotted) and e_g (solid) symmetry at $x=0.2$ (a) and $x=0.4$ (b), respectively. In the DOS of $x=0.4$, the minority spin band of t_{2g} symmetry is shifted slightly above E_F , as compared to the case of $x=0.2$, to make the system half metallic. The DOS of Fig. 3 agrees well with the expected DOS from the double exchange mechanism. The spin-up t_{2g} band is fully occupied and forms localized moment, and the DOS at E_F consists of mainly e_g electrons of Mn- d orbitals. Most notable is that, in the half-metallic regime ($x > 0.33$), the contribution to DOS at E_F comes solely from e_g electrons. This figure indicates that half-metallic electronic structure is consistent with the double exchange mechanism.

The majority spin band of LbMnO_3 yields two Fermi surfaces. They arise from the 19th and the 20th band which correspond to two e_g bands. Since two bands are degenerate along the Γ -R direction, two Fermi surfaces meet at a point of Γ -R line. A large hole Fermi surface centered at R and an electron Fermi surface at Γ are formed by the 19th and the

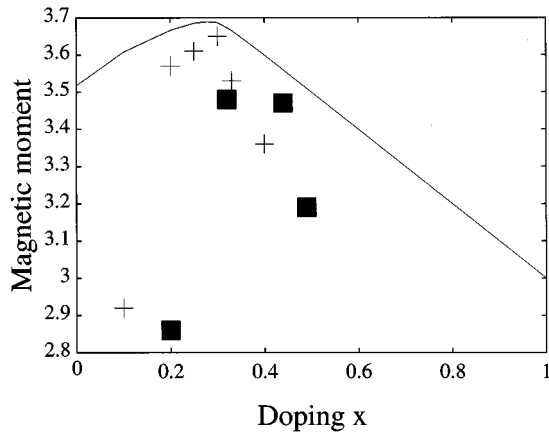


FIG. 4. Calculated magnetic moments as a function of doping concentration. Crosses and squares represent experimental data from Ref. 1 and Ref. 19, respectively.

20th band, respectively. There exist also small majority spin hole Fermi surfaces around R with band indices 16–18. Minority spin electron Fermi surfaces disappear in the half-metallic regime ($x > 0.33$). Topology of the Fermi surface is sensitive to the doping concentration.¹⁸

Calculated magnetic moments of LbMnO_3 , $3.69\mu_B$ and $3.67\mu_B$ for $x = \frac{1}{3}$ and $\frac{1}{4}$, respectively, are close to the experimental values of $3.5\mu_B$ and $3.6\mu_B$.¹⁹ Also, present results of charge occupancies, magnetic moments, and the variation in the energy gap of minority spin band agree, in general, with results of supercell calculations¹³ for $\text{La}_{1-x}\text{Ca}_x\text{MnO}_3$. These agreements reflect that the present calculational scheme gives rise to a reasonable approximation to the real systems. However, there are some minor differences too. The case of $x = \frac{1}{3}$ is half metallic in the present case, while the electronic structure of Pickett and Singh¹³ at $x = \frac{1}{3}$ corresponds to a normal metal albeit nearly half metallic.

Figure 4 shows calculated results of magnetic moment as a function of x , which are compared with experimental values.^{1,19} Calculated magnetic moments here are obtained from the assumed ferromagnetic phase of LbMnO_3 . Hence the comparison of calculated and experimental magnetic moments for $x < 0.2$ is not meaningful, since the real magnetic phase is antiferromagnetic in this regime. In the region of interest $0.2 < x < 0.5$, calculated magnetic moments seem to agree well with experimental ones. There is a peak in magnetic moments near $x \sim 0.3$ which is consistent with experiments. The linear decrease of magnetic moment for $x > 0.33$ can be understood in view of the half-metallic band structure. In the half-metallic $\text{La}_{1-x}\text{Ba}_x\text{MnO}_3$, the minority spin band must be completely filled for all x with an integral number of electrons. Therefore, as the hole doping increases, only the majority spin electrons are depleted so as to reduce the magnetic moment almost linearly with x .

We have studied the change of electronic structure under the magnetic field. The effect of magnetic field is to shift rigidly bands upward or downward according to the direction of spin projection to the magnetic field, without changing the overall shape of band structure. In the inset of Fig. 5, the polarization of LbMnO_3 system is plotted as a function of magnetic field. Here the polarization is defined

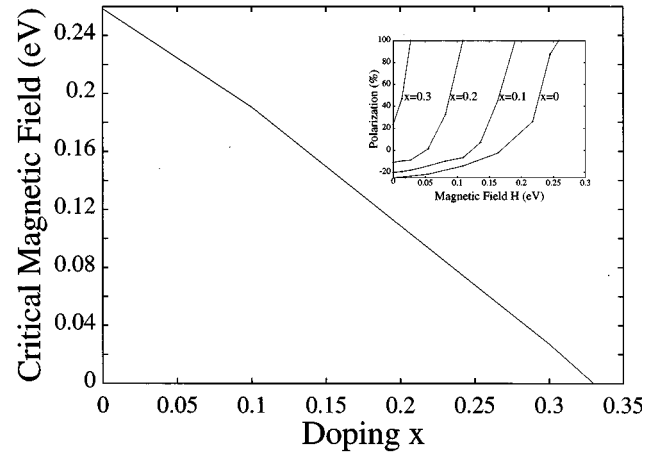


FIG. 5. Phase diagram providing the critical magnetic field H_c in $\text{La}_{1-x}\text{Ba}_x\text{MnO}_3$ as a function of doping concentration x . The upper right corresponds to the half-metallic regime. The inset presents the polarization as a function of magnetic field with varying doping concentration x .

as $P(E_F) = 100 \times \{[N_{\uparrow}(E_F) - N_{\downarrow}(E_F)] / [N_{\uparrow}(E_F) + N_{\downarrow}(E_F)]\}$. The polarization increases with the magnetic field, and at critical magnetic field H_c , the system becomes 100% polarized to become a half metal. This leads to a phase diagram of Fig. 5 providing the critical magnetic field H_c as a function of x . Figure 5 reveals that LaMnO_3 itself becomes half metallic at a field of 0.25 eV ($\sim 4.35 \times 10^3$ T). H_c in the LbMnO_3 system decreases monotonically with x , and H_c is zero for $x > 0.33$. This result suggests that the critical magnetic field H_c becomes small near $x = 0.33$, and so the $\text{La}_{1-x}\text{Ba}_x\text{MnO}_3$ system can be made half metallic even with a laboratory magnetic field.

If the system is fully polarized (100% polarization), the resistivity due to spin-flip scattering will be suppressed.²⁰ In a half metallic system, there is no Stoner continuum to which spins can transit with flipping their spins. It follows that the spin-flip scattering does not contribute to the resistivity in half metallic systems. In this respect, if a system, which is initially not a half-metal, becomes half-metallic by the application of magnetic field or by increasing the doping concentration, the resistivity will decrease dramatically due to a suppression of the spin-flip scattering. Interestingly, the CMR phenomenon in $\text{La}_{1-x}\text{Ba}_x\text{MnO}_3$ is observed at about $x = \frac{1}{3}$, which is near the boundary of the half-metallic transition. In addition, the increase of the polarization is expected to play a role of enhancing MR by contributing tunneling through aligned magnetic domains. By comparing MR's in single and polycrystalline samples, Hwang *et al.*²¹ reported that the spin-polarized transport might be significant in perovskite manganites due to the high degree of spin polarization.

To summarize, we have studied electronic and magnetic properties of $\text{La}_{1-x}\text{Ba}_x\text{MnO}_3$ systematically, by investigating electronic structures of the virtual compound LbMnO_3 . We have also examined the effect of magnetic field on the electronic structure of LbMnO_3 . In the ferromagnetic region $0.2 < x < 0.5$, magnetic properties are well described by this

method. $\text{La}_{1-x}\text{Ba}_x\text{MnO}_3$ becomes half metallic for $x > 0.33$ in the cubic ferromagnetic phase. It is also found that $\text{La}_{1-x}\text{Ba}_x\text{MnO}_3$ even for $x < 0.33$ can be made half metallic by applying the magnetic field. The present study indicates that the half-metallic nature of this system may be responsible for both the linear decrease of the magnetic moment at

high doping concentration and the additional resistivity reduction in the CMR effect.

This work was supported by the Korea Research Foundation, and also in part by the BSRI program of the Korean Ministry of Education and the POSTECH special fund.

-
- ¹E. D. Wollan and W. C. Koehler, *Phys. Rev.* **100**, 545 (1955).
²J. B. A. A. Elemans, B. van Laar, K. R. van der Veen, and B. O. Loopstra, *J. Solid State Chem.* **3**, 238 (1971).
³C. Zener, *Phys. Rev.* **82**, 403 (1951).
⁴P. W. Anderson and H. Hasegawa, *Phys. Rev.* **100**, 675 (1955); P. G. de Gennes, *ibid.* **118**, 141 (1960).
⁵S. Jin, T. H. Tiefel, M. McCormack, R. A. Fastnacht, R. Ramesh, and L. H. Chen, *Science* **264**, 413 (1994).
⁶K. Kubo and N. Ohata, *J. Phys. Soc. Jpn.* **33**, 21 (1972).
⁷R. M. Kusters, J. Singleton, D. A. Keen, R. McGreevy, and W. Hayes, *Physica B* **155**, 362 (1989).
⁸N. Furugawa, *J. Phys. Soc. Jpn.* **63**, 3214 (1994).
⁹A. J. Millis, P. B. Littlewood, and B. I. Shraiman, *Phys. Rev. Lett.* **74**, 5114 (1995); A. J. Millis, B. I. Shraiman, and R. Mueller, *ibid.* **77**, 175 (1996).
¹⁰D. D. Sarma, N. Shanthi, S. R. Barman, N. Hamada, H. Sawada, and K. Terakura, *Phys. Rev. Lett.* **75**, 1126 (1995).
¹¹N. Hamada, H. Sawada, and K. Terakura, *Spectroscopy of Mott Insulators and Correlated Metals*, Springer Series in Solid-State Science Vol. 119 (Springer-Verlag, Berlin, 1995).
¹²S. Satpathy, Z. S. Popović, and F. R. Vukajlović, *Phys. Rev. Lett.* **76**, 960 (1996).
¹³W. E. Pickett and D. J. Singh, *Phys. Rev. B* **53**, 1146 (1996).
¹⁴N. Hamada, H. Sawada, and K. Terakura, *J. Phys. Chem. Solids* **56**, 1719 (1995).
¹⁵W. H. Butler, X.-G. Zhang, and J. M. MacLaren, in *Magnetic Ultrathin Films, Multilayers, and Surfaces*, edited by E. E. Marinero *et al.*, MRS Symposium Proceedings No. 384 (Materials Research Society, Pittsburgh, 1995), pp. 439–443.
¹⁶W. E. Pickett and D. J. Singh, *Phys. Rev. B* **55**, R8642 (1997).
¹⁷R. von Helmolt, J. Wecker, B. Holzapfel, L. Schultz, and K. Samwer, *Phys. Rev. Lett.* **71**, 2331 (1993).
¹⁸S. J. Youn and B. I. Min (unpublished).
¹⁹G. H. Jonker and J. H. Van Santen, *Physica (Amsterdam)* **16**, 337 (1950).
²⁰V. Yu. Irkhin and M. I. Katsnel'son, *Usp. Fiz. Nauk* **164**, 705 (1994) [*Sov. Phys. Usp.* **37**, 659 (1994)].
²¹H. Y. Hwang, S.-W. Cheong, N. P. Ong, and B. Batlogg, *Phys. Rev. Lett.* **77**, 2041 (1996).